Can we delineate hydrocarbon bearing zones using magnetotelluric technique?

K.S. Ajithabh, Cochin University of Science and Technology, Kerala*
Prasanta K. Patro#, CSIR-National Geophysical Research Institute, Hyderabad
Ujjal K. Borah, CSIR- National Geophysical Research Institute, Hyderabad
*ajithabhks@gmail.com
#corresponding author (patrobpk@ngri.res.in)

Keywords

Magnetotellurics, Hydrocarbon, Sub-basalt

Summary

The present study aims to analyze whether the hydrocarbon bearing zones within a sedimentary strata can be delineated through magnetotelluric (MT) approach or not. For that a synthetic model is created taking inputs from well log data (resistivity log) of a hydrocarbon producing zone. Synthetic data is generated from this model and then inverted to test the ability of MT for identification of hydrocarbon bearing zones. The resolution enhancement criteria proposed by recent study is also applied to increase the resolution of the inversion output. But in the inversion output of this model, hydrocarbon bearing zones are not identified. The reasons for this inability of detection are then studied in terms of thickness of the hydrocarbon bearing zone and the conductivity of the overburden taking different situations. Finally, the study finds that the detectability of hydrocarbon bearing zone is controlled by the thickness of the zone and conductivity of overburden.

Introduction

The magnetotellurics (MT) is a passive electromagnetic geophysical method proposed by the Cagniard(1953). Though initially it was extensively applied in the crustal studies all over the world wide spread research in MT proved that it could delineate the sedimentary structures below the resistive layers such as carbonates, volcanics and overthrusts (Anderson & Pelton, 1985; Berkman & Orange, 1985; Orange, 1989). Hence it opened a new lap in the global hydrocarbon exploration.

The major chunk of petroleum deposits are deep buried within the Mesozoic sediments and generally their presence is scanned by the seismic reflection method. But the highly complex structure of the basalts limits the seismic reflections from sub-basaltic layers due to scattering and generation of multiples, hence reducing its efficiency to delineate the sub-basaltic sediments (Yilmaz, 2001; Ziolkowski et al., 2001). Extensive studies in MT had proved it to be the best method for sub-basalt explorations. The modelling studies from available well log data verified the efficacy of the MT method to delineate the sub-basaltic Mesozoic sediments (Patroetal., 2015).The study demonstrated the sub-basaltic Mesozoic sediments could directly be identified from the MT modelling if the top layer is basalt and constrained modelling is necessary if the basalt overlays by a conductive layer. Several hydrocarbon explorations had been conducted in various regions of the world using MT (Sarvandani et al, 2017; Berdichevsky, et al., 2015; Mansoori et al., 2015; Colombo et al., 2011; Abdul Azeez et al., 2011; Pandey et al., 2009; Khalil & Ushijima, 2003; Mitsuhata et al., 1999; Christopherson, 1991; Stanley et al., 1985) in the basaltic, carbonate and overthrust scenarios. Though the existing studies could delineate the sedimentary structure which act as reservoir formation, the hydrocarbon bearing zones could not identified by the MT.

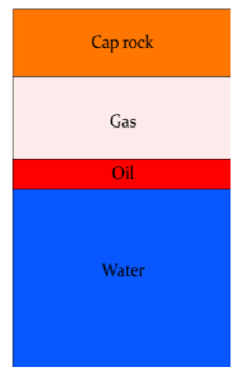

Figure 1: Arrangement of hydrocarbon in reservoir.

The aim of the present study is to examine whether MT can delineate the hydrocarbon bearing zones. The subsurface deposits of hydrocarbons are arranged in a specific manner depending on their density as shown in figure 1. The gas is seen on top followed by oil and water respectively. Hydrocarbon deposits are sealed by a particular rock type namely, cap rock which conceals its escape from reservoir. Hence it is an essential factor for the petroleum occurrence. Shale, anhydrite and evaporates are the common cap rocks. Our present study is based on the thickness and resistivity values obtained from well log data ofa hydrocarbon producing zone. 1D base model of the hydrocarbon producing zone is constructed on the basis of this well log datafor the forward study and the synthetic data is generated. 1D modelling of the synthetic data was carried out to study the efficiency of MT to delineate the hydrocarbon bearing zones. The suggestions from the study by Borah and Patro (2017) are employed in our study to enhancing the resolution of MT.

Methodology

2.1 Forward modelling

Well logging is a geophysical method which measures the insitu rock properties by drilling boreholes. In view of the hydrocarbon exploration the measured rock properties are resistivity, density, porosity. As true resistivity is the ultimate result of the MT, the resistivity information from the well log is very useful for the MT forward modelling stuidies.

Laterolog Deep (LLD)is a resistivity tool in well logging which measures the closest true formation resistvity (Serra, 1984). So, we have used the LLD values of a producing well for our study (data is obtained by personal communication). The data is smoothened employing the spline method (de Boor, 1978) using MATLAB and the general trend in resistivity of different zones are obtained. Table 1 provides the thickness, resistivity and interpreted information of the different zones from the well log.

Thickness (m)	*Resistivity (Ωm)*	*Type*
60	*1*	*Shale*
50	*15*	*Carbonate laminations: Gas bearing zone*
50	*700*	*Massive cabonates: Gas bearing zone*
20	*20*	*Oil leg of the gas cap*
140	*2*	*Water bearing zone*

Table 1: Thickness and resistivity of the formations and their interpretation obtained from the well log.

Informations of the overlying layers above the hydrocarbon bearing zones were not available in the well log and it is necessary for MT studies. As data was not available, we assumed the top layer as basalt of thickness 1 km, underlying the mesozoic sediments of thickness 1 km andfollowed by the basement. The hydrocarbon beaing zones are present within the mesozoic sediments. The resistivity values assignedfor the basalt, mesozoic and basement are 100 Ωm, 10 Ωm and 1000 Ωm respectively. Using these parameters (layer thickness and resistivity) and the parameters from well log data the 1D base model for forward study is constructed (figure 2a). After that, synthetic data is generated from this model using figure 2b, 2c). This synthetic data is used for further studies.

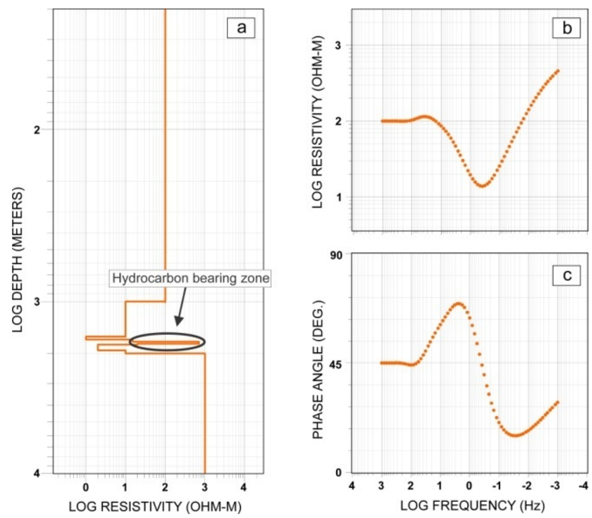

Figure 2: a) Base model constructed based on the information from the resistivity well log for the forward modelling. b) Synthetic resistivity data obtained from the forward modelling of the base model c) Synthetic phase data obtained from the forward modelling of the base model

2.2 Inversion of the synthetic data

During the inversion of the synthetic data, the evaluation (target) frequency separation is taken according to the criterion suggested by Borah and Patro, 2017. The study of Borah and Patro, 2017 has quantitatively proved that the resolution of the layers (both resistivity and thickness) can be enhanced if the evaluation (target) frequency separation (Δf) is less than or equal to a threshold value; which is 0.141

times of the lowest frequency (f_n) to be used (equation 1).

$$\Delta f \le 0.414\, f_n \qquad (1)$$

Therefore, in the present studywe have sampled the evaluation (target) frequencies at the rate of $0.2\, f_n$ with $f_n = 0.01$ Hz to invert the synthetic data.

First, the synthetic data is inverted using Occam 1D inversion scheme (Constable et al., 1987) which produced a smoothly varying multi-layered model of the synthetic data. From this multilayered model the input model (with minimum number of layers) is fixed and Marquardt inversion (Marquardt, 1963) is run to get a maximum fit of the model response with the synthetic data. The Marquardt inversion (Marquardt, 1963) assembles the fine fit of the model with the synthetic data by employing maximum neighborhood method. The final model derived from the Marquardt inversion and its fitted responses are shown in figure 3.

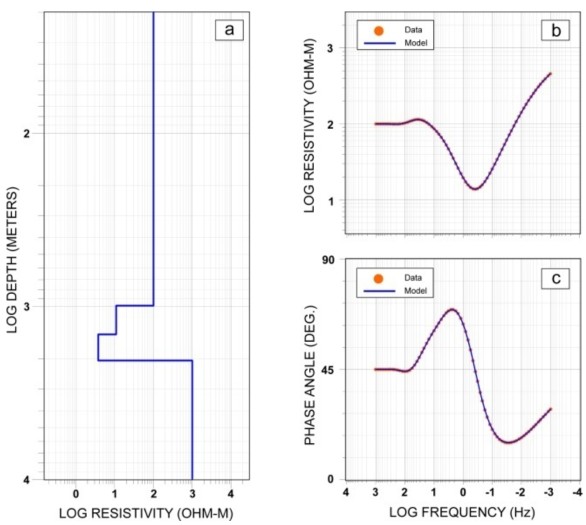

Figure 3: a) 1D inverted model of the synthetic data. b, c) The model fit with the data

Again, according to Patro et al., 2015, constrained inversion of the MT data can enhance the output. So, we have carried out the constrained inversion of our synthetic data set to get an enhanced result by fixing the basaltic layer and leaving all other parameters free. But the constrained inversion could not improve the earlier result.

Discussion

The main objective of the study was to test whether the hydrocarbon bearing zone is detectable or not. The hydrocarbon bearing zones (figure2a) are composed of a resistor (700 Ωm) represents the gas bearing zone and the underlying low resistive (20 Ωm) layer represents the oil bearing zone (Table 1). But the final model could not resolve these gas and oil bearing zones, instead the model brings out a conductor of resistivity 3 Ω m which do not represent any signature of hydrocarbon. But the reason for this weakness is to be identified. So, we tried to find out the reason behind it on the basis of minimum resolvable layer thickness proposed by Borah and Patro, 2017. The minimum layer thickness that can be resolved, below a certain depth, with two adjacent frequencies is given by (Borah and Patro, 2017) –

$$t > 0.169\sqrt{d_n^a}\sqrt{d_m^a} \qquad (2)$$

where d_n^a is the skin depth for frequency f_n with apparent resistivity ρ_n^a and d_m^a is the skin depth for frequency f_m with apparent resistivity ρ_m^a.

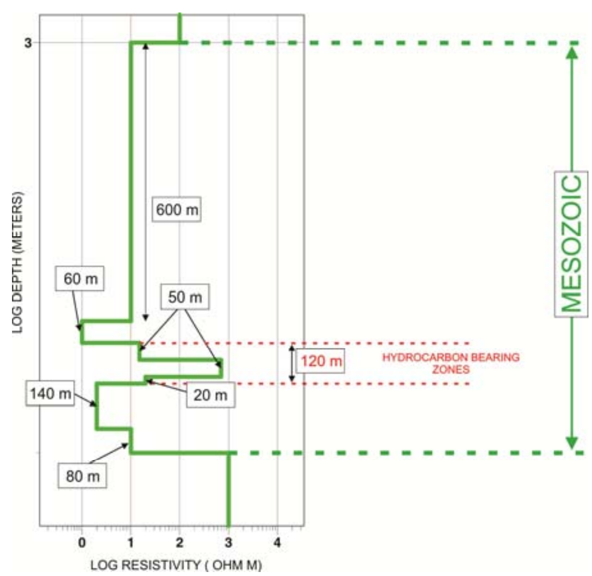

Figure 4: Detailed view of the hydrocarbon bearing zones. The thickness of each layers are shown in boxes.

Now, the geological formation of our interest begins from 1660 m as shown in figure 4 (enlarged view of figure 2a). So, to obtain the minimum resolvable layer thickness below depth 1660 m, we have calculated the corresponding evaluation (target) frequencies (for our data set) on the basis of skin depth. We have found that frequency 7 Hz provides a skin depth of 1624 m (<1660 m) and adjacent frequency 5.9 Hz provides a skin depth of 1702 m (>1660 m). So, we have taken this 7 Hz and its adjacent lower frequency 5.9 Hz to calculate the minimum resolvable layer thickness. Now, putting these skin depth values in equation (2) we have the minimum resolvable layer thickness below 1660 m as –

$$t > 0.169\sqrt{1624}\sqrt{1702} \quad (3)$$

$$t > 281\, m \quad (4)$$

This implies that the thickness of the layer below 1660 m should be more than 281 m and then it will be resolved by MT. But, in our case, the hydrocarbon bearing layers has thickness less than 281 m and so, it is not delineated. In the final output model (Figure 3a), the layer of thickness 417 m with resistivity of 3 Ω m is delineated instead of hydrocarbon bearing zones. So, the layers distinguished in the final model (figure 3a) are the basaltic layer on top followed by the Mesozoic layer, the conductive layer and then the basement.

This result implies that the thickness of the layer is a factor for the delineation in MT. From equation (4) we observed that the hydrocarbon bearing zone should be more than 281 m in order to resolve by the MT. Therefore, we tested this thickness criterion by increasing the thickness of the 700 Ω m resistive layer of the base model (figure 2a) to 300 m (figure 5a). The synthetic data is generated for this model and this data is inverted using Occam inversion (Constable et al., 1987) to assign the input model for Marquardt inversion (Marquardt, 1963). The final inverted model obtained after Marquardt inversion (Marquardt, 1963) could resolve a conductive layer and not any information of the resistive layer (figure 5b).

This led to a new insight that the resolution of the layers depends not only on the thickness in this case. The other factors may be the conductivity of the overburden; as conductive overburden decreases the resolution of the underlying resistor relative to the background resistivity which is known as the screening effect and the resistive overburden can enhance the resolution of the underlying conductor (Bedrosian, 2007).

So, we tested this overburden scenario by embedding two layers of thickness 500 m, in which one layer is highly resistive (700 Ωm) and other is highly conductive (1 Ωm) into a common background of 100 Ωm. First, we put the conductive layer over the resistive layer (figure 6a) and synthetic data is generated from it. Figure 6b shows the final inverted model obtained from this synthetic data. The resistive layer beneath the conductor is not resolved in this case. Then we repeated the procedure by putting the

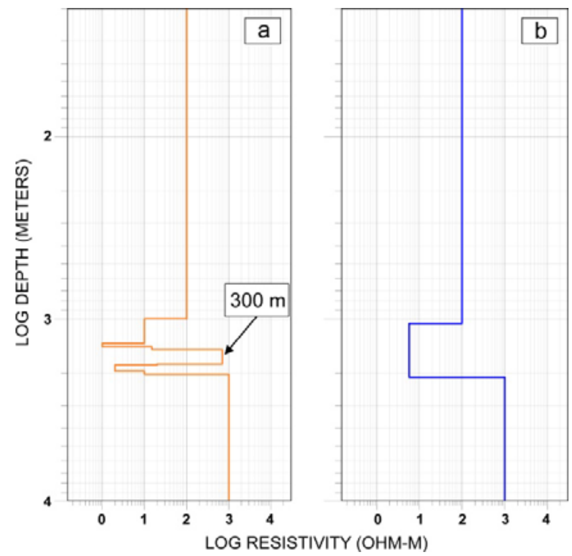

Figure 5:a) The base model created for the forward modeling studies. b) 1D inverted model of the synthetic data generated from the base model shown in 5a.

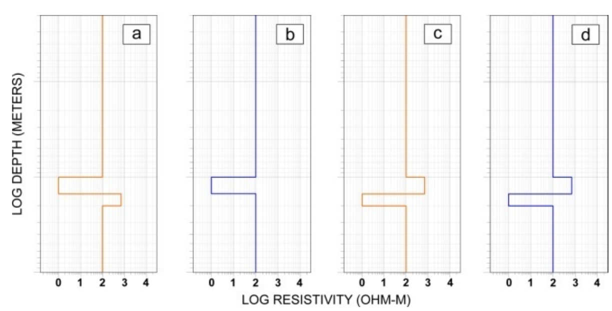

Figure 6: a) Base model for the forward modelling studies. b) 1D inverted model of the synthetic data obtained from the model 6a. c) Base model for the forward modelling studies. d) 1D inverted model of the synthetic data obtained from the model 6c

resistive layer as the overburden (figure 6c), the synthetic data is generated on it and then inverted. The inverted model is presented in figure 6d. It is clear from the model that the conductive layer just beneath the resistive overburden is resolved. For both the cases we have applied the same evaluation (target) frequency separation. So, this study brings out the screening effect of the deeper conductive layer.

It is evident that the overlying conducting layers hides the thin resistive layers beneath it. The sedimentary structures are generally conducting in nature. Though the resistive hydrocarbon bearing zones are occurring in sediments, they are hidden in MT output due to the screening effect of sedimentary rocks. In our present scenario, the hydrocarbon bearing zones are overlain by the highly conducting (1 Ωm) shale and then the remaining Mesozoic sediment above it with resistivity of 15 Ωm. Therefore, the resistive hydrocarbon bearing zones could not be identified by the MT due to the screening effect of the sediments.

Conclusions

The main motto of the present study was to test the efficiency of MT in delineating the different hydrocarbon bearing zones within a sedimentary formation. The study is started with a synthetic model which is constructed on basis of well log information from a producing well. For this model, MT was unable to resolve the hydrocarbon bearing zones. The cause behind this weakness is studied on the basis of conductivity of overburden and thickness of hydrocarbon bearing zone. The study finds that if the over burden conductivity is too high then it is difficult to get the below layers through MT as the input energy cannot penetrated much below due the screening effect. If the overburden is moderately conductive or resistive then the hydrocarbon bearing layers can be delineated by MT. But, in this case thickness of the hydrocarbon bearing zone plays an important role and it should have a certain threshold thickness as suggested by Borah and Patro (2017). In our case, the overburden of HC bearing layer is high conductive shale (1 Ohm.m). So, it acts as a shield to the beneath hydrocarbon bearing zones and it is not detected through MT. If the overburden is moderately conductive then there are possibilities to detect the hydrocarbon layers if the layers fulfill the thickness criteria.

Acknowledgments

KSA thanks to Director, CSIR-NGRI for giving permission to work in NGRI. KSA thanks Dr. K. Sajan, Head of Department, Department of Marine Geology and Geophysics for giving opportunity to carry out dissertation work in CSIR-NGRI. All colleagues from MT & DRS division, CSIR-NGRI are gratefully acknowledged. Research of PKP and UKB was funded through the project MLP-6104-28(BPKP).

References

Abdul Azeez, K. K., Satish Kumar, T., Basava, S., Harinarayana, T., & Dayal, A. M. (2011). Hydrocarbon prospects across Narmada-Tapti rift in Deccan trap, central India: Inferences from integrated interpretation of magnetotelluric and geochemical prospecting studies. *Marine and Petroleum Geology, 28* , 1073-1082.

Anderson, R., & Pelton, W. H. (1985). MT Exploration In Volcanic Cover, Overthrust Belts, And Rift Zones. *Society of Exploration Geophysicists* .

Bedrosian, P. A. (2007). MT+, integrating magnetotellurics to determine earth structure, physical state, and processes. *Surveys in Geophysics* , 121-167.

Berdichevsky, M. N., Bubnov, V., Aleksanova, E., Alekseev, D., Yakovlev, A., & Yakovlev, D. (2015). Chapter 13 – Magnetotelluric Studies in Russia: Regional-Scale Surveys and Hydrocarbon Exploration. *Electromagnetic Sounding of the Earth's Interior (Second Edition)* , 379–401.

Berkman, E., & Orange, A. (1985). Interesting aspects of magnetotelluric data in Northwestern Montana. *SEG Technical Program Expanded Abstracts* , 271-274.

Borah, U. K., & Patro, P. K. (2017). Effect of evaluation frequency separation on magnetotelluric resolution. *ANNALS OF GEOPHYSICS* , G0330.

Cagniard, L. (1953). Basic theory of the Magnetotelluric method of Geophysical prospecting. *GEOPHYSICS* , 605-635.

Christopherson, K. R. (1991). Applications of magnetotellurics to petroleum exploration in Papua New Guinea : A model for frontier areas. *The Leading Edge, 10(4)* , 21-27.

Colombo, D., Keho, T., Janoubi, E., & Soyer, W. (2011). Sub-basalt imaging with broadband magnetotellurics in NW Saudi Arabia. *SEG Annual Meeting* , 619-623.

Constable, S. C., Parker, R. L., & Constable, a. C. (1987). Occam's inversion: A practical algorithm for generating smooth models from electromagnetic sounding data. *Geophysics* , 289-300.

de Boor, C. (1978). A Practical Guide to Splines. *Springer-Verlag, New York* .

Khalil, A., & Ushijima, K. (2003). Magnetotelluric Soundings in Minami-Noshiro Oil Field, Japan. *Memoirs of the Faculty of Engineering, Kyushu University 63(2)* , 87-106.

Mansoori, I., Oskooi, B., & Pedersen, L. B. (2015). Magnetotelluric signature of anticlines in Iran's Sehqanat oil field. *Tectonophysics, 654* , 101-112.

Marquardt, D. W. (1963). An Algorithm for Least-Squares Estimation of Nonlinear Parameters. *Journal of the Society for Industrial and Applied Mathematics* , 431-441.

Mitsuhata, Y., Matsuo, K., & Minegishi, M. (1999). Magnetotelluric survey for exploration of a volcanic-rock reservoir in the Yurihara oil and gas field, Japan. *Geophysical Prospecting* , 195-218.

Orange, A. S. (1989). Magnetotelluric Exploration for Hydrocarbons. *Proceedings of the IEEE* , 287-317.

Pandey, D., Singh, S., Sinha, M., & MacGregor, L. (2009). Structural imaging of Mesozoic sediments of Kachchh, India, and their hydrocarbon prospects. *Marine and Petroleum Geology* , 1043-1050.

Patro, P. K., Abdul Azeez, K. K., Veeraswamy, K., Sarma, S. V., & Sen, M. K. (2015). Sub-basalt sediment imaging - The efficacy of magnetotellurics. *Journal of Applied Geophysics* , 106-115.

Sarvandani, M. M., Kalateh, A. N., Unsworth, M., & Majidi, A. (2017). Interpretation of magnetotelluric data from the Gachsaran oil field using sharp boundary inversion. *Journal of Petroleum Science and Engineering* , 25-39.

Serra, O. (1984). *Fundamentals of well-log interpretation, 1. the acquisition of well-log data.* Elsevier.

Stanley, W. D., Saad, A. R., & Ohofugi, W. (1985). Regional Magnetotelluric Surveys in Hydrocarbon Exploration, Parana Basin, Brazil. *American Association of Petroleum Geologists Bulletin, 69(3)* , 346-360.

Yilmaz, O. (2001). *Seismic Data Analysis, Processing, Inversion and Interpretation of Seismic Data. Investigations in Geophysics No. 10, .* Society of Exploration Geophysicists vol. II.

Ziolkowski, A., Hanssen, P., Gatliff, R. L., & Jakubowicz, H. (2001). The use of low frequencies for sub-basalt imaging. (pp. 74-77). 71st Ann. Internat. Mtg.